# Electronic Structure and Photoionization and Dissociation Processes of Bis(trifluoromethoxy)disulfurylperoxide, $CF_3OS(O)_2OOS(O)_2OCF_3$

**Maofa Ge,*,† Li Yao,†,‡ and Dianxun Wang†**

*State Key Laboratory for Structural Chemistry of Unstable and Stable Species, Beijing National Laboratory for Molecular Sciences (BNLMS), Institute of Chemistry, Chinese Academy of Sciences, Beijing, 100080, People's Republic of China, and Graduate School of Chinese Academy of Sciences, Beijing, 100039, People's Republic of China*

*Received: July 9, 2007; In Final Form: October 16, 2007*

In this work, we present a complete study of the photoionization and dissociation processes for bis(trifluoromethoxy)disulfurylperoxide, $CF_3OS(O)_2OOS(O)_2OCF_3$, which was generated by UV photolysis of a mixture of $(CF_3CO)_2O$, $SO_2$, and $O_2$ at a low temperature. The reaction product was detected and characterized by the photoelectron (PE) and photoionization mass spectroscopy (PIMS). For comparison, the geometric and electronic structures of $CF_3S(O)_2OS(O)_2CF_3$ (**a**), $CF_3OS(O)_2OS(O)_2OCF_3$ (**b**), and $CF_3OS(O)_2OOS(O)_2OCF_3$ (**c**) were investigated by the combination of experiments and theoretical studies. The PES results show that the outer electrons residing in $n_{O(S=O)}$ of **b** and **c** are more tightly bound than those of **a**. It is worthwhile mentioning that drastic changes occur in the geometry of **c** after one-electron ionization. The neutral molecule exhibits a gauche structure with the SOOS dihedral angle of 124.4°. The first ionization process happens on the O−O antibonding orbital. The remarkable geometric changes between the ground-state molecule and cation are computed to be the gauche-to-trans rotation of $\delta_{SOOS}$ and the prolongation of the S1−O1 single bond length. According to the calculated bond dissociation energies, the dissociation process was discussed. The calculated results indicate that once the parent ion is formed, the dissociation of the S1−O1 bond to form $CF_3OSO_2^+$ is inevitable.

## Introduction

It is now well-established that atomic chlorine, transported to the stratosphere by a variety of particularly stable chlorine-containing compounds, is responsible for the catalytic destruction of ozone in that region of the atmosphere.[1] As substitutes for one class of these stable compounds, the chlorofluorocarbons (CFCs) and various hydrochlorofluorocarbons (HCFCs) and hydrofluorocarbons (HFCs) are presently being considered. The essential advantage shared by the proposed substitutes with respect to their ozone depletion potentials is their incomplete halogenation. The carbon−hydrogen bonds present in HCFCs and HFCs are prone to attack by tropospheric OH radicals, a reaction which produces a water molecule and a haloalkyl radical.[2]

The trifluoromethyl radical, $CF_3$, is expected to be an intermediate in the atmospheric oxidation process of several of the compounds proposed as substitutes for CFCs.[2] Under atmospheric conditions, the immediate fate of this radical (as for other alkyl radicals) is the addition of an oxygen molecule to form the corresponding alkylperoxy radical.[3,4] As with other peroxy radicals ($RO_2$) the atmospheric fate of $CF_3O_2$ radicals is reaction with NO, $NO_2$, $HO_2$, or other peroxy radicals. The reaction with $NO_2$ gives trifluoromethyl peroxynitrate.[5,6] $CF_3OONO_2$ may serve as a reservoir molecule for either $CF_3O$ or $NO_2$ radicals, which may contribute to the depletion of ozone in the stratosphere or to the transport of $NO_2$ from industrial zones into otherwise pollution-free environments.[7,8] However, other reactions of $CF_3O_2$ radicals are usually neglected because of the low concentrations of possible reaction partners or comparably slow reaction rates.

Nonetheless, one atmospheric species that has been largely ignored until recently is $SO_2$.[9] The abundance of $SO_2$ in the atmosphere is highly variable. Its concentrations can reach levels of 1000 ppb.[10] The reaction of $CF_3O$ with $SO_2$ has been shown to produce the $CF_3OSO_2$ radical. Francisco and von Ahsen[9] present the first direct spectroscopic identification of the $CF_3OSO_2$ radical isolated in an inert-gas matrix generated by reaction of $CF_3O$ radicals with $SO_2$, which demonstrates the existence of the first link between $C_nF_mO_y$ species and $SO_x$ in the atmosphere. One expected atmospheric fate of the $CF_3OSO_2$ radical is the rapid reaction with molecular oxygen leading to the peroxy radical $CF_3OS(O)_2OO$. Peroxy radicals readily convert to the corresponding oxy radicals under atmospheric conditions. This is done by rapid reaction with trace gases such as NO, CO, or ozone;[11] consequently, it is expected that $CF_3OSO_2$ forms $CF_3OSO_3$ in the atmosphere. The first spectrosopic evidence for the existence of the $CF_3OSO_3$ radical has been obtained through the low-pressure flash thermolysis experiments of highly diluted $CF_3OS(O)_2OOS(O)_2OCF_3$.[12] The peroxide was prepared by UV photolysis of a mixture of $(CF_3CO)_2O$, $SO_2$, and $O_2$ held at −40 °C.

In earlier studies of atmospheric species containing $CF_3$ group, we reported the gas-phase electronic structures of $CM_3C(O)ONO$, $CM_3C(O)ONO_2$ (M = H, Cl, F), $CF_3OONO_2$, and $CF_3C(O)OSSOC(O)CF_3$.[13−15] The aim of this work is to conduct the photochemical reaction of $CF_3$ radical with $SO_2$ and $O_2$ to isolate the short-time intermediate $CF_3OS(O)_2OOS(O)_2OCF_3$

* To whom correspondence should be addressed. E-mail: gemaofa@iccas. ac.cn.

† Institute of Chemistry, Chinese Academy of Sciences.

‡ Graduate School of Chinese Academy of Sciences.

10.1021/jp0753326 CCC: $37.00 
Published on Web 12/05/2007

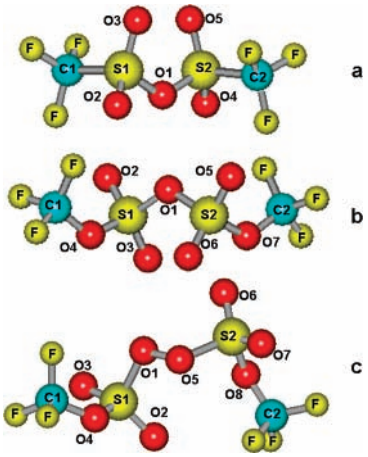


**Figure 1.** Molecular models of (a) $CF_3S(O)_2OS(O)_2CF_3$, (b) $CF_3OS(O)_2OS(O)_2OCF_3$, and (c) $CF_3OS(O)_2OOS(O)_2OCF_3$.

and to characterize it by spectroscopic techniques. The possible ionization and dissociation processes are investigated. For comparison of the experimental results, the geometric and electronic structures (Figure 1) of $CF_3S(O)_2OS(O)_2CF_3$ (**a**), $CF_3OS(O)_2OS(O)_2OCF_3$ (**b**), and $CF_3OS(O)_2OOS(O)_2OCF_3$ (**c**) were investigated by the photoelectron (PE) and photoionization mass spectroscopy (PIMS) with the help of theoretical calculations.

## Experimental Section

**Synthesis of $CF_3OS(O)_2OS(O)_2OCF_3$ and $CF_3OS(O)_2OOS(O)_2OCF_3$ and Reagents.** $CF_3OS(O)_2OOS(O)_2OCF_3$ was synthesized by mixing 6 mbar of $(CF_3CO)_2O$, 20 mbar of $SO_2$, and $O_2$ up to 1 atm in a 5 L photoreactor, maintained at −40 °C, and subjecting the mixture to 254 nm radiation for about 6 h. Lowering the temperature to −50 °C allows evaporation of the volatile compounds, as there are the excess oxygen and $SO_2$, unreacted perfluoroacetic anhydride, and $COF_2$ as the product of a minor side reaction. Peroxide **c** is further purified by trap-to-trap condensation, where it proved to be immobile in a trap held at −40 °C [12] before detection with the photoelectron and photoionization mass spectrometer.

$CF_3OS(O)_2OS(O)_2OCF_3$ was synthesized when the above reaction was maintained at 0 °C, which is identified by its known mass spectrum.[16]

As $CF_3$ radical source, perfluoroacetic anhydride was chosen, because its absorption cross-section at the emission line of the mercury lamp at 254 nm is quite high. Perfluoroacetic anhydride (Alfa-Aesar), trifluoromethanesulfonic anhydride (**a**, Alfa-Aesar) were obtained from commercial sources and used without further purification.

**Instrumentation.** The experimental apparatus used in this work has been described previously.[17,18] Briefly, the photoelectron and photoionization mass spectrometer consists of two parts: one part is the double-chamber UPS-II machine; another part is a time-of-flight mass spectrometer. The photoelectron spectrum was recorded on the double-chamber UPS-II machine which was built specifically to detect transient species at a resolution of about 30 meV, as indicated by the $Ar^+(^2P_{2/3})$ photoelectron band.[19,20] Experimental vertical ionization energies are calibrated by simultaneous addition of a small amount of argon and methyl iodide to the sample. Mass analysis of ions is achieved with the time-of-flight mass analyzer mounted directly to the photoionization point. The relatively soft ionization is provided by single-wavelength HeI radiation. The PE and PIMS spectra can be recorded within seconds of each other under identical conditions.

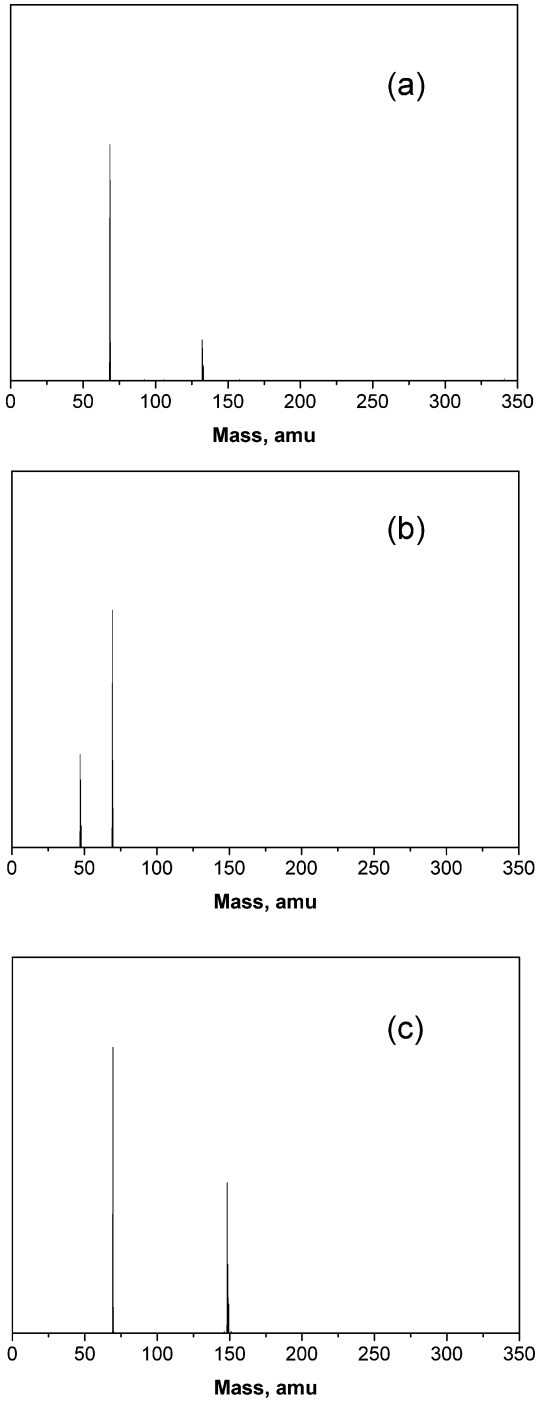


**Figure 2.** HeI photoionzation mass spectra of (a) $CF_3S(O)_2OS(O)_2CF_3$, (b) $CF_3OS(O)_2OS(O)_2OCF_3$, and (c) $CF_3OS(O)_2OOS(O)_2OCF_3$.

**Quantum Chemical Calculation.** Electronic property calculations were carried out using the Gaussian series of programs.[21] Because the values and the order of the MO energies depend on the molecular geometry, the calculations of the geometries of the neutral ground state were performed by using density functional theory (B3LYP) at the 6-311+G* basis set. Vibrational frequency calculations have been carried out to verify stationary points. The relaxed scans of the potential energy surface were performed at HF/6-31G* and B3LYP/6-31G* levels before the geometric optimization. To assign the PE spectrum, the outer-valence Green's function (OVGF) calculations[22,23] at the 6-31G basis set, which include sophisticated

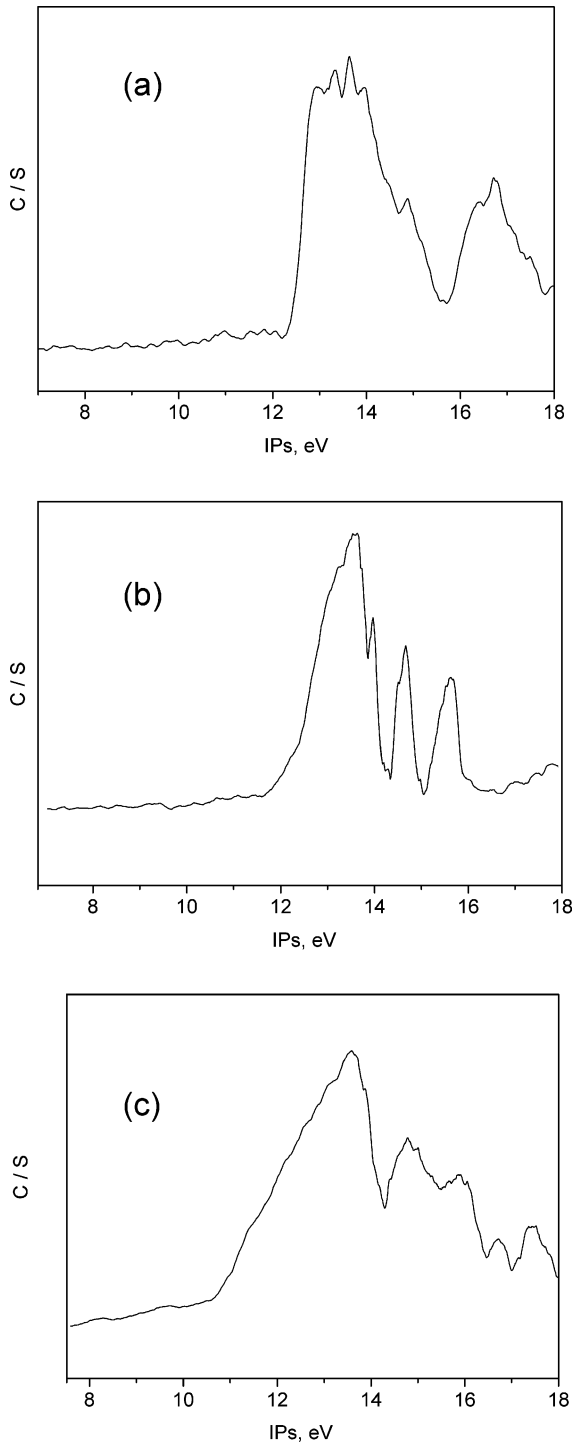


**Figure 3.** HeI photoelectron spectra of (a) $CF_3S(O)_2OS(O)_2CF_3$, (b) $CF_3OS(O)_2OS(O)_2OCF_3$, and (c) $CF_3OS(O)_2OOS(O)_2OCF_3$.

correlation effects of the self-energy, were applied to the molecules to give results of the vertical ionization energies. The energetics of the dissociation of the parent ion into possible fragments were also calculated at the B3LYP/6-311+G* level of theory.

## Results and Discussion

The PIMS and PES results of **a**, **b** and **c** are shown in Figures 2 and 3, respectively. The photoionization mass spectra are relatively simple. For **a**, it has two peaks at $m/z = 69$ and 133. For **b**, the two peaks are at $m/z = 47$ and 69. They are in agreement with previously reported values.[16,24] But peroxide **c** obtained at low temperature shows a different spectrum. A new peak for $CF_3OS(O)_2^+$ at $m/z = 149$ in Figure 2c replaces the peak at $m/z = 47$ in Figure 2b. In the PES, the first PE band is a broad band for compounds **a**−**c**. The ionization and dissociation processes are discussed in detail later. First, the molecular geometries and electronic structures are investigated and presented as following.

**TABLE 1: Selected Bond Distances (Å) and Angles (deg) for a−c**

| Compound **a** ($C_2$) | | |
|---|---|---|
| | B3LYP/6-311++G** | GED[a] |
| S1−O1 | 1.690 | 1.623(5) |
| S1−O2 | 1.438 | 1.409(3) |
| S1−C1 | 1.902 | 1.848(6) |
| O1−S1−O2 | 104.4 | 104.6(11) |
| O1−S1−O3 | 110.8 | 109.6(11) |
| O2−S1−O3 | 124.2 | 128.0(21) |
| S1−O1−S2 | 130.1 | 128.1(14) |
| O1−S1−C1 | 96.97 | 99.1(14) |
| S1−O1−S2−C2 | 96.23 | 99.1(14) |
| Compound **b** ($C_2$) | | |
| | B3LYP/6-311++G** | GED[a] |
| S1−O1 | 1.673 | |
| S1−O2 | 1.430 | |
| S1−O4 | 1.653 | |
| O4−C1 | 1.397 | |
| O1−S1−O2 | 103.4 | |
| O1−S1−O3 | 109.8 | |
| O2−S1−O3 | 125.7 | |
| S1−O1−S2 | 127.0 | |
| O1−S1−O4 | 99.82 | |
| S1−O4−C1 | 123.0 | |
| O1−S1−O4−C1 | 82.78 | |
| O4−S1−O1−S2 | 72.36 | |
| Compound **c** ($C_1$) | | |
| | neutral | cation |
| S1−O1 | 1.680 | 2.035 |
| S1−O2 | 1.429 | 1.423 |
| S1−O4 | 1.654 | 1.591 |
| C1−O4 | 1.397 | 1.475 |
| O1−O5 | 1.452 | 1.280 |
| O1−S1−O2 | 101.9 | 99.47 |
| O1−S1−O3 | 110.6 | 102.4 |
| O2-S1-O3 | 126.3 | 129.7 |
| S1−O1−O5 | 110.0 | 111.2 |
| O1−S1−O4 | 100.2 | 93.88 |
| S1−O4−C1 | 123.1 | 123.7 |
| C1−O4−S1−O1 | 80.63 | 90.36 |
| O4−S1−O1−O5 | 63.49 | 108.5 |
| S1−O1−O5−S2 | 124.4 | 180.0 |
| O1−O5−S2−O8 | 72.42 | 108.5 |
| O5−S2−O8−C2 | 89.19 | 90.36 |

[a] Reference 25.

**Molecular Geometries.** Geometry optimizations for **a**−**c** were performed using the density functional theory (DFT) method, and the selected geometric parameters were given in Table 1.

Results of gas electron diffraction (GED) reveal that molecule **a** possesses a skew structure with $C_2$ symmetry and a SOSC dihedral angle of 99.1(14)°.[25] The structure obtained by theoretical methods is in good agreement with the GED experimental results.

The starting geometries of the conformers of **b** and **c** for quantum chemical calculations were based on the structure of **a** measured by GED since there are no experimental data on the structures of **b** and **c**. Before the geometric optimization, relaxed scans of the potential energy surface were performed

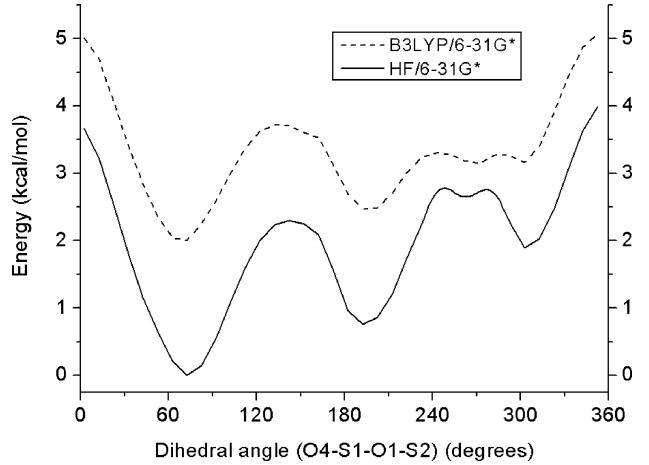


**Figure 4.** Calculated potential curves for internal rotation around the S1−O1 bond in **b** at the HF/6-31G* and B3LYP/6-31G* levels. The curve of B3LYP/6-31G* level is shifted by 2 kcal/mol.

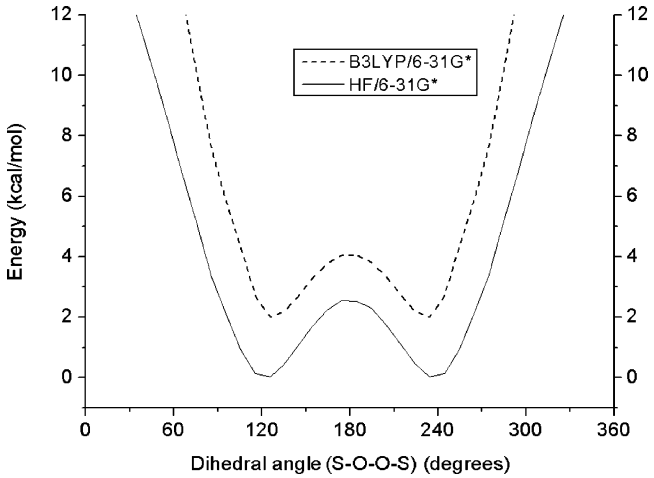


**Figure 5.** Calculated potential curves for internal rotation around the O−O bond in **c** at the HF/6-31G* and B3LYP/6-31G* levels. The curve of the B3LYP/6-31G* level is shifted by 2 kcal/mol.

for internal rotation around the S1−O1 bond of **b** and the O1−O5 bond of **c** at HF/6-31G* and B3LYP/6-31G* levels. Figures 4 and 5 show the calculated potential curves for dihedral angles $\delta_{O4S1O1S2}$ of **b** and $\delta_{S1O1O5S2}$ of **c**, respectively. As seen from Figure 5, there are two minima of the calculated potential curves at both levels, which indicate the existence of a stable conformer with the gauche structure and with $\delta_{S1O1O5S2}$ around 120 or 240°. The situation of **b** in Figure 4 is different, which shows that besides the gauche structure with $\delta_{O4S1O1S2}$ around 70°, a pseudo trans structure probably also exists as a stable conformer. But the energy of the pseudo trans conformer is higher (0.5−0.75 kcal/mol) than the gauche conformer. So our discussion of the geometry and electronic structure of **b** and **c** mainly focuses on the gauche conformer for simplicity.

From the optimized geometries for the gauche structures of **b** and **c** (shown in Table 1), we can see that the S1−O1 and S1−O4 bonds are the typical S−O single bond (1.60−1.69 Å) and the S1−O2 bond is a typical S═O double bond (1.40−1.45 Å). Molecule **b** possesses a gauche structure with $C_2$ symmetry and the O4S1O1S2 dihedral angle of 72.4°. The predicted O−O bond length (1.452 Å) of **c** is close to that of the molecules HOOH (1.464(3) Å),[26] $CH_3OOCH_3$ (1.457(12) Å),[27] and $FO_2SOOSO_2F$ (1.455(13) Å).[28] Besides the O−O bond length, another important structural parameter for peroxides is the dihedral angle of $\delta_{ROOR}$, which can influence the overall structure of the molecules greatly. Because of the lone pair−lone pair interactions, **c** adopts a gauche conformation as the most stable structure. The dihedral angle of $\delta_{SOOS}$ in **c** (124.4°) is between those of $FO_2SOOSO_2F$ (119(5)°)[28] and $F_5SOOSF_5$ (129(2)°),[29] which could be illustrated by the steric interaction of the moieties.

**TABLE 2: Experimental and Calculated Vertical Ionization Potentials and MO Characters for a−c**

| compd | | $E_i$ | GF | MO | character |
|---|---|---|---|---|---|
| a | 1 | 12.97 | 12.99 | 35a | $n_{O(S=O,S-O-S)}$ |
| | 2 | 13.28 | 13.13 | 34b | $n_{O(S=O)}$ |
| | 3 | | 13.20 | 33b | $n_{O(S=O)}$ |
| | 4 | 13.62 | 13.45 | 34a | $n_{O(S=O)}$ |
| | 5 | | 13.62 | 33a | $n_{O(S=O)}$ |
| | 6 | | 13.65 | 32b | $n_{O(S=O)}$ |
| | 7 | 13.95 | 13.88 | 31b | $n_{O(S=O,S-O-S)}$ |
| | 8 | 14.87 | 14.80 | 30b | $n_{O(S-O-S)}$ |
| b | 1 | 13.60 | 13.84 | 39a | $n_{O(S=O,S-O-S)}$ |
| | 2 | | 13.91 | 38b | $n_{O(S=O)}$ |
| | 3 | | 13.97 | 37b | $n_{O(S=O,S-O-S)}$ |
| | 4 | | 14.06 | 38a | $n_{O(S=O)}$ |
| | 5 | 14.01 | 14.34 | 37a | $n_{O(S-O-C)}$ |
| | 6 | 14.66 | 14.63 | 36b | $n_{O(S=O)}$ |
| | 7 | | 14.66 | 35b | $n_{O(S=O)}$ |
| c | 1 | 13.62 | 13.83 | 81 | $n_{O(S=O)}$ |
| | 2 | | 13.88 | 80 | $n_{O(S=O)}$ |
| | 3 | | 13.90 | 79 | $n_{O(S=O)}$ |
| | 4 | | 14.00 | 78 | $n_{O(S=O,OO)}$ |
| | 5 | | 14.01 | 77 | $n_{O(S=O)}$ |
| | 6 | | 14.13 | 76 | $n_{O(S=O)}$ |
| | 7 | 14.77 | 14.55 | 75 | $n_{O(S-O-C)}$ |
| | 8 | | 14.64 | 74 | $n_{O(S-O-C)}$ |

The geometric parameters of the cation-radical conformer of **c** are fully optimized with the DFT method. After the vibrational analysis, the calculated results show that the radical cation with pseudo $C_i$ symmetry is a local minimum. The remarkable geometric changes between **c** and its ground-state cation are computed to be a gauche-to-trans rotation around the O−O bond ($\delta_{S1O1O5S2}$ from 124.4 to 180.0°) and a prolongation of the S1−O1 single bond length by 0.35 Å (Table 1). Both structural changes upon ionization are embodied in the PE and PIMS spectra of **c**.

**Photoelectron Spectra.** The HeI photoelectron spectra of **a**−**c** are shown in Figure 3. The PES experimental vertical ionization energies, the theoretical vertical ionization energies, and the molecular orbital (MO) characters of the outer valence shells from the OVGF calculations are listed in Table 2.

The high electronegativity and chemical reactivity of the trifluoromethylsulfonyl group are well-known.[30−32] There has been a rapid growth in the chemistry of the corresponding anhydride **a**.[33−35] Its IR,[36] NMR,[37] mass spectrum,[16] and gas electron diffraction[25] were thoroughly investigated. However, there was no photoelectron spectroscopy investigation before. In the present study, the photoelectron spectrum of **a** was measured for comparison with **b** and **c** obtained from the photochemical reaction of $CF_3$ radical with $SO_2$ and $O_2$.

As seen from Figure 3a, the HeI photoelectron spectrum of **a** exhibits a group of broad bands in the low-energy region (<15.5 eV). The experimental vertical ionization energies listed in Table 2 are in good agreement with the calculated values with the OVGF method. By comparison with $X_2SO_2$ (X = $CH_3$, F, Cl),[38,39] one would expect these IPs corresponding roughly to the oxygen lone pairs. The first vertical ionization energy is located at 12.97 eV. This band is assigned to the removal of an electron from the highest occupied molecular orbital (HOMO), which is mainly characterized by the lone pairs of the oxygen atom from S═O and S−O−S. The second and third bands

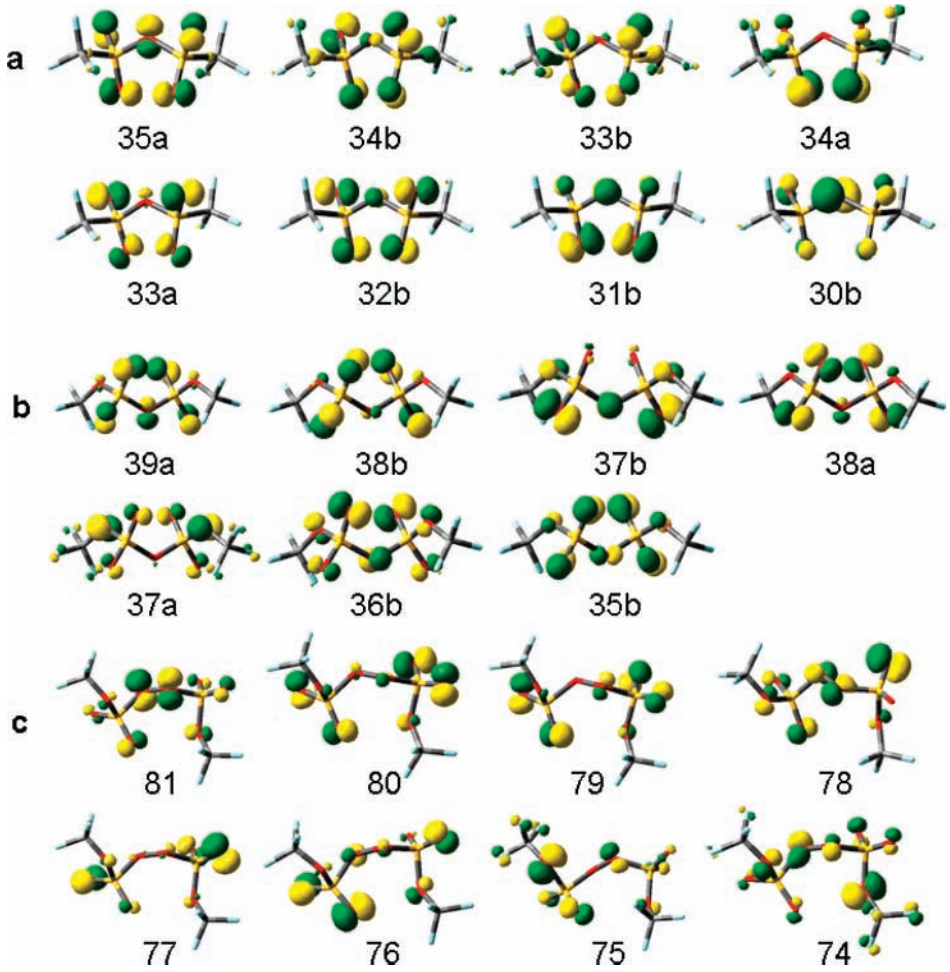


**Figure 6.** Characters of the outer occupied molecular orbitals for **a**−**c**.

(13.28 and 13.62 eV) are the results of the removal of the electron of the lone pairs of $O_{(S=O)}$. This character is similar to the molecule $SO_2F_2$, of which the first band at 13−14 eV is ascribed to the oxygen lone pair of $O_{(S=O)}$.[40] The next band at 13.95 eV comes from the ionization process of $\{31b(n^B_{O(S=O,S-O-S)})\}^{-1}$. In the low-energy region, the last band centered at 14.87 eV is attributed to the ionization of the electron in the nonbonding orbitals of the oxygen atom in the S−O−S bond.

A similar analysis can be done for the assignment of the HeI photoelectron spectrum of **b** and **c**. Drawings of the outer occupied molecular orbitals are given in Figure 6. Combined with theoretical calculations, the assignment of the bands in the photoelectron spectra could be easily done.

According to the ROVGF calculations (Table 2) and population analysis (Figure 6), the character of the HOMO of **b** corresponds to the lone pair of $n_{O(S=O,S-O-S)}$. It is consistent with the HOMO of **a**. In Figure 3b, the first band centered at 13.60 eV is attributed to the ionization processes of $\{39a\ (n^A_{O(S=O,S-O-S)})\}^{-1}$, $\{38b\ (n^B_{O\ (S=O)})\}^{-1}$, $\{37b\ (n^B_{O(S=O,S-O-S)})\}^{-1}$, and $\{38a\ (n^A_{O(S=O)})\}^{-1}$. According to the results of theoretical calculations, these four IPs are very close and could not be clearly distinguished under our experimental conditions. While the following band centered at 14.01 eV is sharper and clear. It is due to the removal of the electron of the lone pair of $O_{(S-O-C)}$, which is absent in the character of the oxygen lone pair of **a**. Furthermore, when the $CF_3$ moiety in **a** is replaced by the $CF_3O$ moiety in **b**, the first PE band shifts to higher ionization energy region, which means that the lone pair electron of $O_{(S=O,S-O-S)}$ atom in **b** tends to be more difficult to ionize. As for the band at 14.66 eV, it is also attributed to the ionization of the electron from the oxygen lone pair of the S═O double bond and also higher than the corresponding one in **a**.

Peroxide **c** has a high density of ionic states, which results in many overlapping bands in the PE spectrum (Figure 3c). In fact, this spectrum looks like the spectrum of the monoxide **b** with more overlapped bands. With combined empirical and theoretical analysis, it is found that the first PE band of c centered at 13.62 eV corresponds to the overlapping of six ionizations from the oxygen lone pair of O−O and S═O. The calculated first adiabatic and vertical ionization energies are 10.68 and 13.84 eV, respectively. The second PE band centered at 14.77 eV is assigned to come from the removal of an electron of $n_{O(S-O-C)}$. The ionization energies of **c** at the high ionization energy region between 15.0 and 18.0 eV have not been attributed.

In conclusion, the outer electrons of **a**−**c** most reside in the oxygen lone pairs of S═O, and those of **b** and **c** are more tightly bound than **a** because of the influence of the substituted groups.

**Ionization and Dissociation of c.** One of the main proposes of this work is to investigate the ionization and dissociation processes of **c**. The neutral ground state of **c** possesses the $C_1$ symmetry. Drastic changes occur in the geometry of **c** after one-electron ionization.

An interesting and important feature of **c** is the change of the SOOS dihedral angle and the O−O single bond length, which are the geometric parameters most influenced by the removal of electron from the HOMO, O−O antibonding orbital. Usually, the ionization of antibonding orbital would increase the bonding nature. It is just the case for the O−O single bond, which is theoretically calculated to be 0.17 Å shorter after

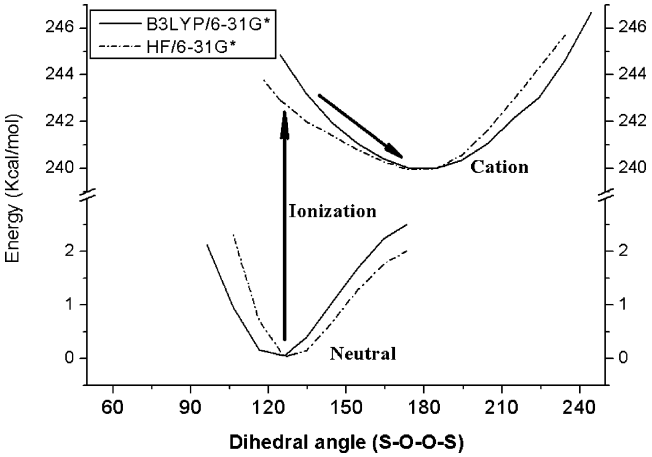


**Figure 7.** Potential curves for internal rotation around the O−O bond of **c** in the neutral and cation-radical conformers calculated at the HF/6-31G* and B3LYP/6-31G* levels. The cationic curve of the HF/6-31G* level is shifted by 8 kcal/mol.

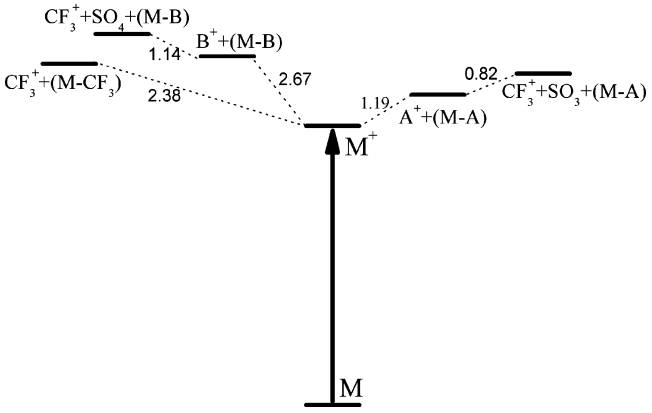


**Figure 8.** Schematic energy profile showing ionization and dissociation pathways of **c** calculated at the B3LYP/6-311+G* level of theory in electronvolts (M = $CF_3OS(O)_2OOS(O)_2OCF_3$, A = $CF_3OS(O)_2$, and B = $CF_3OS(O)_2O$).

ionization. The relaxed scan of the potential energy surface for internal rotation around the O−O bond in the neutral and cation-radical conformers was calculated through structure optimizations at the SOOS dihedral angle. In Figure 7, both B3LYP and HF methods with small basis set (6-31G*) predict that the internal rotation of the SOOS dihedral angle occurs after ionization, and the cation-radical structure possesses a pseudo $C_i$ symmetry with the SOOS dihedral angle of 180°. This change in the geometry may be the reason for the structureless broad band observed when the first ionization process occurs. After the original study performed by Walsh,[41] many workers[42−44] have published qualitative and quantitative MO studies using Walsh diagrams. Thus, they have been able to predict geometry differences between the ground and ionized states. Erben and Della Védova investigated the cation-radical geometry using full ab initio calculations. It was observed that drastic changes occur in the geometry of both $FC(O)SSCH_3$ and FC(O)SSSC(O)F after ionization.[45]

In the cation-radical structure of **c**, another important change of the geometry is the remarkably prolonged S1−O1 single bond. It suggests that the parent ion prefers the dissociation of the S1−O1 single bond to form $CF_3OSO_2^+$. The possible dissociation pathways for **c** are presented in Figure 8. As can be seen, the energy for the heterolysis of parent ion to $A^+$ (A = $CF_3OS(O)_2$) is much lower than that of homolysis to $B^+$ (B = $CF_3OS(O)_2O$). The quite low energy for the S1−O1 bond dissociation in the parent ion suggests that once the parent ion is formed, dissociation into $CF_3OSO_2^+$ is very easy. This fact explains the absence of the parent ion and the appearance of $CF_3OSO_2^+$ in the PIMS (Figure 2c). Besides, peak $CF_3^+$ can be formed by the subsequent dissociation of $CF_3OSO_2^+$ as well as by direct dissociation of C−O in the parent ion. From Table 1, we can see that the C1−O4 bond of **c** also has the trend of prolongation after ionization.

## Conclusion

$CF_3OS(O)_2OOS(O)_2OCF_3$ was generated by UV photolysis of a mixture of $(CF_3CO)_2O$, $SO_2$, and $O_2$ at low temperature. The product was detected and characterized by the PES and PIMS. For comparison, the geometric and electronic structures of **a**−**c** were investigated by the combination of experiments and theoretical studies. The PES results show that the outer electrons of **a**−**c** most reside in $n_{O(S=O)}$, and those of **b** and **c** are more tightly bound than **a** because of the influence of the substituted groups. It is worthwhile mentioning that drastic changes occur in the geometry of **c** after one-electron ionization. The molecule exhibits a typical gauche structure observed in other peroxides, with the $\delta_{SOOS}$ dihedral angle of 124.4°. The first ionization process happens on the O−O antibonding orbital. The remarkable geometric changes between the ground-state molecule and cation are computed to be the gauche-to-trans rotation of $\delta_{SOOS}$ and the prolongation of the S1−O1 single bond length. According to the calculated bond dissociation energies, the dissociation process is discussed. The calculated results indicate that once the parent ion is formed, the dissociation of the S1−O1 bond forming $CF_3OSO_2^+$ is easy to occur.

**Acknowledgment.** This project was supported by the Knowledge Innovation Program (Grant No. KZCX2-YW-205) and Hundred talents fund of the Chinese Academy of Sciences, the 973 Program (No. 2006CB403701) and the 863 Program (No. 2006AA06A301) of the Ministry of Science and Technology of China, and the National Natural Science Foundation of China (Contract Nos.20577052, 20673123, 20473094, and 20503035). L.Y. thanks the Chinese Academy of Sciences for a scholarship during the period of this work.

## References and Notes

(1) Rowland, F. S. *Annu. Rev. Phys. Chem.* **1991**, *42*, 731.
(2) Wallington, T. J.; Schneider, W. F.; Worsnop, D. R.; Nielsen, O. J.; Sehested, J.; DeBruyn, W.; Shorter, J. A. *Environ. Sci. Technol.* **1994**, *28*, 320.
(3) Ryan, K. R.; Plumb, I. C. *J. Phys. Chem.* **1982**, *86*, 4678.
(4) Caralp, F.; Lesclaux, R.; Dognon, A. M. *Chem. Phys. Lett.* **1986**, *129*, 433.
(5) Hohorst, F. A.; DesMarteau, D. D. *Inorg. Chem.* **1974**, *13*, 715.
(6) Kopitzky, R.; Willner, H.; Mack, H.-G.; Pfeiffer, A.; Oberhammer, H. *Inorg. Chem.* **1998**, *37*, 6208.
(7) Ko, M. K. W.; Sze, N.-D.; Rodriguez, J. M.; Weisenstein, D. K.; Heisey, C. W. *Geophys. Res. Lett.* **1994**, *21*, 101.
(8) Becker, K. A.; Mayer-Figge, A. *Ber.−Bergische Univ. Gesamthochsch. Wuppertal, Fachbereich 9, Phys. Chem.* **1997** (42), 1−158.
(9) von Ahsen, S.; Francisco, J. S. *Angew. Chem., Int. Ed.* **2004**, *43*, 3330.
(10) Uherek, E. Atmospheric trace gas mixing ratios. Max Planck Institut für Chemie, Mainz, Germany; www.atmosphere.mpg.de/enid/25i.html (accessed 2004).
(11) von Ahsen, S.; Willner, H.; Argüello, G. A. *J. Fluorine Chem.* **2004**, *125*, 1057.
(12) von Ahsen, S, Francisco, J. S. *J. Phys. Chem. A* **2005**, *109*, 9193.
(13) Zeng, X.; Yao, L.; Wang, W.; Liu, F.; Sun, Q.; Ge, M.; Sun, Z.; Zhang, J.; Wang, D. *Spectrochim. Acta, Part A* **2006**, *64*, 949.
(14) Yao, L.; Du, L.; Ge, M.; Wang, D. *J. Chem. Phys.* **2007**, *126*, 184301.
(15) Zeng, X.; Ge, M.; Sun, Z.; Wang, D. *J. Phys. Chem. A* **2006**, *110*, 5685.

(16) van Meter, W. P.; Cady, G. H. *J. Am. Chem. Soc.* **1960**, *82*, 6005.
(17) Yao, L.; Zeng, X. Q.; Ge, M. F.; Wang, W. G.; Sun, Z.; Du, L.; Wang, D. X. *Eur. J. Inorg. Chem.* **2006**, 2469.
(18) Wang, W. G.; Yao, L.; Zeng, X. Q.; Ge, M. F.; Sun, Z.; Wang, D. X. *J. Chem. Phys.* **2006**, *125*, 234303.
(19) Chunhui, L.; Gongyi, H.; Benming, C.; Dianxun, W.; Peel, J. *B. J. Phys. Chem. A* **1998**, *102*, 3877.
(20) Chunhua, Q.; Gongyi, H.; Dianxun, W. *J. Phys. Chem. A* **1999**, *103*, 1972.
(21) Frisch, M. J.; Trucks, G. W.; Schlegel, H. B.; Scuseria, G. E.; Robb, M. A.; Cheeseman, J. R.; Montgomery, J. A., Jr.; Vreven, T.; Kudin, K. N.; Burant, J. C.; Millam, J. M.; Iyengar, S.; Tomasi, J.; Barone, V.; Mennucci, B.; Cossi, M.; Scalmani, G.; Rega, N.; Petersson, G. A.; Nakatsuji, H.; Hada, M.; Ehara, M.; Toyota, K.; Fukuda, R.; Hasegawa, J.; Ishida, M.; Nakajima, T.; Honda, Y.; Kitao, O.; Nakai, H.; Klene, M.; Li, X.; Knox, J. E.; Hratchian, H. P.; Cross, J. B.; Adamo, C.; Jaramillo, J.; Gomperts, R.; Stratmann, R. E.; Yazyev, O.; Austin, A. J.; Cammi, R.; Pomelli, C.; Ochterski, J.; Ayala, P. Y.; Morokuma, K.; Voth, G. A.; Salvador, P.; Dannenberg, J. J.; Zakrzewski, V. G.; Dapprich, S.; Daniels, A. D.; Strain, M. C.; Farkas, O.; Malick, D. K.; Rabuck, A. D.; Raghavachari, K.; Foresman, J. B.; Ortiz, J. V.; Cui, Q.; Baboul, A. G.; Clifford, S.; Cioslowski, J.; Stefanov, B. B.; Liu, G.; Liashenko, A.; Piskorz, P.; Komaromi, I.; Martin, R. L.; Fox, D. J.; Keith, T.; Al-Laham, M. A.; Peng, C. Y.; Nanayakkara, A.; Challacombe, M.; Gill, P. M. W.; Johnson, B.; Chen, W.; Wong, M. W.; Andres, J. L.; Gonzalez, C.; Replogle, E. S.; Pople, J. A. *Gaussian 03*, revision B.01; Gaussian, Inc.: Pittsburgh, PA, 2003.
(22) Ortiz, J. V. *J. Chem. Phys.* **1988**, *89*, 6348.
(23) von Niessen, W.; Schirmer, J.; Cederbaum, L. S. *Comp. Phys. Rep.* **1984**, *1*, 57.
(24) Olah, G. A.; Weber, T.; Farooq, O. *J. Fluorine Chem.* **1989**, *43*, 235.
(25) Haist, R.; Mack, H.-G.; Waterfeld, A.; Gard, G. L.; Oberhammer, H. *J. Mol. Struct.* **1996**, *380*, 213.
(26) Khachkuruzov, G. A.; Przhevalskii, I. N. *Opt. Spectrosc.* **1974**, *36*, 299.
(27) Hass, B.; Oberhammer, H. *J. Am. Chem. Soc.* **1984**, *106*, 6146.
(28) Hagen, K.; Hedberg, K.; Gard, G.; Aubke, F. *J. Mol. Struct.* **2001**, *1*, 567.
(29) Zylka, P.; Oberhammer, H.; Seppelt, K. *J. Mol. Struct.* **1991**, *243*, 411.
(30) Senning, A. *Chem. Rev.* **1996**, *65*, 385.
(31) Howells, R. D.; McCown, T. D. *Chem. Rev.* **1977**, *77*, 69.
(32) Hendrickson, T. B.; Sternback, D. D.; Bair, K. W. *Acc. Chem. Res.* **1977**, *10*, 306.
(33) Lu, J.-Y.; Arndt, H.-D. *J. Org. Chem.* **2007**, *72*, 4205.
(34) Zhou, H.-B.; Liu, G.-S.; Yao, Z.-J. *Org. Lett.* **2007**, *9*, 2003.
(35) Varghese, O. P.; Barman, J.; Pathmasiri, W.; Plashkevych, O.; Honcharenko, D.; Chattopadhyaya, J. *J. Am. Chem. Soc.* **2006**, *128*, 15173.
(36) Gramstad, T.; Haszeldine, R. N. *J. Chem. Soc.* **1957**, 4069.
(37) Stang, P. J.; Dueber, T. E. *Org. Synth.* **1974**, *54*, 79.
(38) Solouki, B.; Bock, H.; Appel, R. *Angew. Chem, Int. Ed. Engl.* **1972**, *11*, 927.
(39) Solouki, B.; Bock, H.; Appel, R. *Chem. Ber.* **1975**, *108*, 897.
(40) Chadwick, D.; Frost, D. C.; Herring, F. G.; Katrib, A.; McDowell, C. A.; McLean, R. A. N. *Can. J. Chem.* **1973**, *51*, 1893.
(41) Walsh, A. D. *J. Chem. Soc.* **1953**, *3*, 2260.
(42) Gillbro, T. *Phosphorus Sulfur Relat. Elem.* **1978**, *4*, 133.
(43) Kimura, K.; Osafune, K. *Bull. Chem. Soc. Jpn.* **1975**, ***48***, 2421.
(44) Gimarc, B. M. *J. Am. Chem. Soc.* **1970**, *92*, 266.
(45) Erben, M. F.; Della Védova, C. O. *Inorg. Chem.* **2002**, *41*, 3740.